



# Assimilating All-Sky Microwave Radiance Data to Improve NASA GEOS Forecasts and Analysis

Min-Jeong Kim, Jianjun Jin, Amal El Akkraoui, Ricardo Todling,  
Wei Gu, Will McCarty, and Ron Gelaro

**NASA Global Modeling and Assimilation Office (GMAO)**



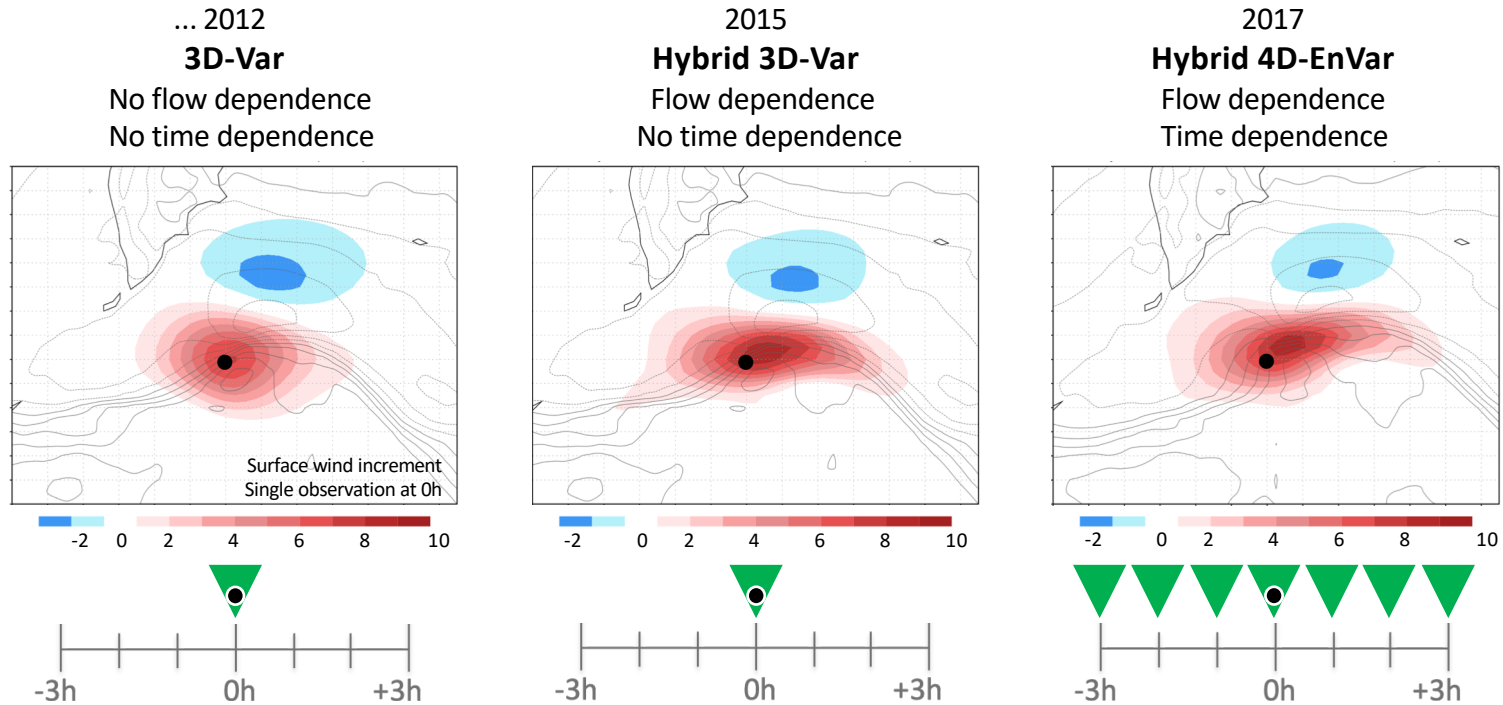
## NASA Global Modeling and Assimilation Office (GMAO) and Goddard Earth Observing System (GEOS)

- ❑ The GMAO is an organization that performs research, develop models and assimilation systems, and produce quasi-operational products to support NASA's Earth Science missions.
  
- ❑ We use Goddard Earth Observing System (GEOS) which is the main system that is used for applications across a wide range of spatial scales, from kilometers to many tens of kilometers. The system consists of a group of model components such as
  - Atmospheric General Circulation Model (AGCM)
  - Ocean General Circulation Model (OGCM)
  - Chemistry-Climate Model (CCM)
  - Chemistry Transport Model (CTM)

# GEOS Atmospheric Data Analysis System (ADAS)

Is currently based on hybrid 4D-EnVar configuration of GSI

## Evolution of the GEOS data assimilation methodology



Courtesy: Amal El Akkraoui

In 2017, GEOS data assimilation algorithm was upgraded to Hybrid 4D-EnVar which allowed the analysis changes to be flow dependent and time dependent. Therefore, situation dependent analysis forcing from observation data are now applied to the model forecasts.



# Data Currently Assimilated In GEOS Forward Processing (FP) System

- AMSU-A
  - MHS
  - ATMS
  - SSMIS
  - All-sky GMI
- Passive Microwave Radiometers**
- AIRS
  - IASI
  - HIRS
  - CrIS
  - AVHRR
  - SEVIRI
  - GOES
- Passive Infrared Radiometers**
- Conventional Data : Sonde, Buoy, Ship data, Aircraft data
  - GPS Radio Occultation : refractivity
  - OMI, MLS ozone data
  - SatWind retrieved wind vectors



# Data Currently Assimilated In GEOS FP System

All-sky MHS and all-sky AMSR2 will be implemented in GEOS-FP later this year

- AMSU-A
- **MHS**
- ATMS
- SSMIS
- **All-sky GMI**

**In GEOS-FP since July 2018**

Passive Microwave Radiometers

- AIRS
- IASI
- HIRS
- CrIS
- AVHRR
- SEVIRI
- GOES

Passive Infrared Radiometers

- Conventional Data : Sonde, Buoy, Ship data, Aircraft data
- GPS Radio Occultation : refractivity
- OMI, MLS ozone data
- SatWind retrieved wind vectors



## Assimilation of cloud- and precipitation-affected radiances

- Significant changes were made in GEOS to assimilate cloud and precipitation affected radiance data (Kim et al. 2020, MWR).
- **Four new state and analysis control variables** were added for hydrometeors (liquid cloud, ice cloud, rain, and snow)
- **Background error** for these hydrometeors are generated and used.
- **Observation error** models (symmetric error model, Geer and Bauer 2011) were built and tuned.
- **Bias correction** and **quality control** procedures for all-sky microwave radiance data were developed.
- **Enhanced radiance observation operator**, Community Radiative Transfer Model (CRTM)

## Improving Radiance Observation Operator

In CRTM, optical properties for microwave wavelengths are read from a lookup table. In integrating radiative transfer processes, CRTM uses these optical properties and water contents for hydrometeors to compute the optical depth ( $\tau$ ) contributed from each cloud type in an atmospheric layer.

$$\tau = \rho \times k_e$$

where  $\rho$  is integrated cloud water content for a layer ( $\text{kg}/\text{m}^2$ ) provided as input and  $k_e$  is mass extinction coefficient ( $\text{m}^2/\text{kg}$ ) calculated using the CRTM lookup table.



## Improving Radiance Observation Operator

### Improvement 1: Reconstructed CRTM cloud scattering coefficients needed as part of the GSI observation operator

- Analogous to Geer and Baordo (2014), optical properties of 11 different non-spherical ice crystal shapes in Liu (2008) database were examined to find an optimal choice of ice crystal shape.
- For each shape of ice crystal, a CRTM cloud coefficient lookup table was generated for 33 microwave frequencies between 10.65 GHz and 190.31 GHz, seven atmospheric temperatures between 243 K and 303 K, and 405 effective radius sizes starting from 0.005 mm.

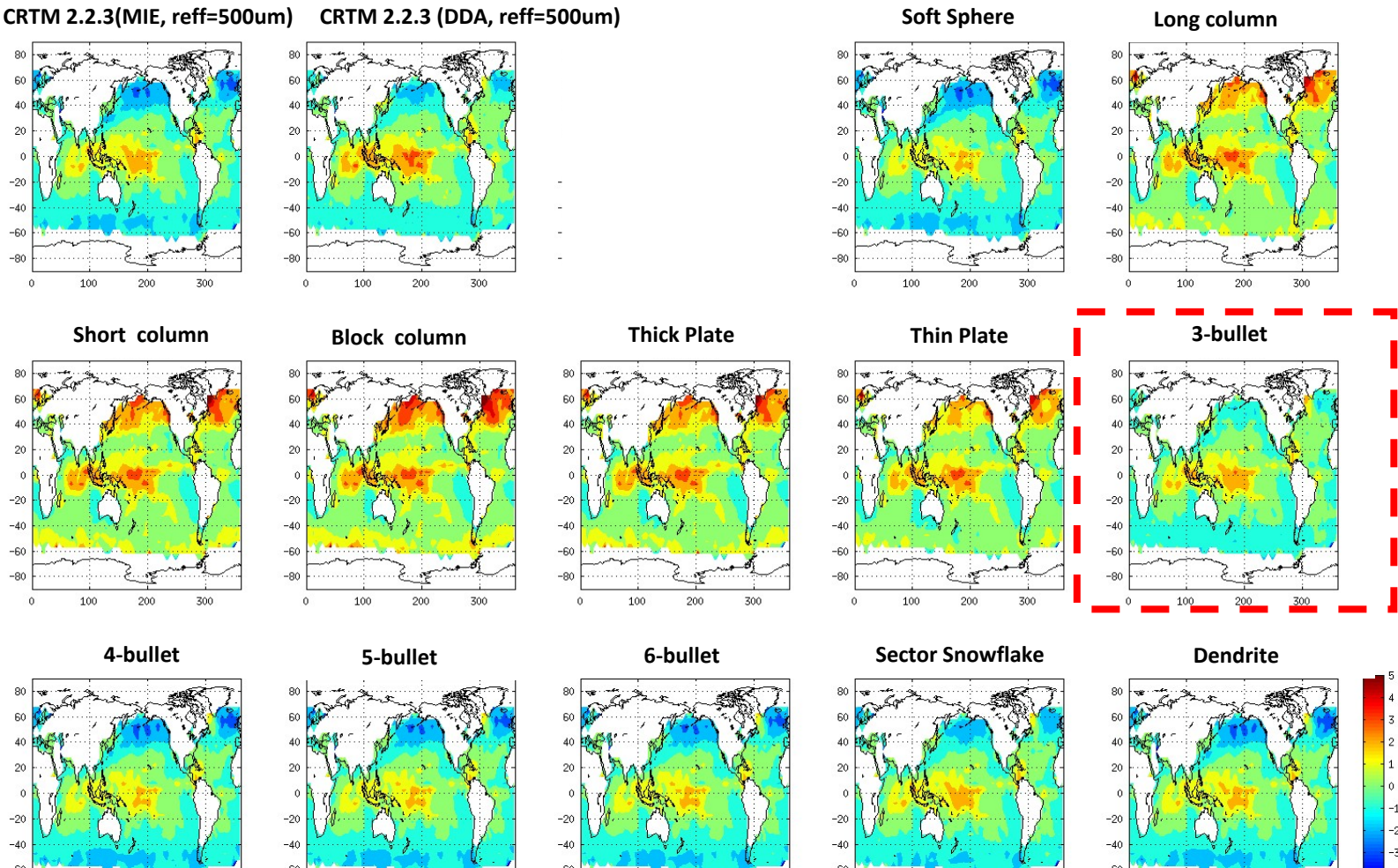
### Improvement 2: Enhanced consistency in $R_{\text{eff}}$ between CRTM inputs and CRTM lookup table

- CRTM requires users to provide effective radius and water content as inputs. Using the input effective radius and the input sensor's frequency, CRTM calculates optical properties by interpolating scattering coefficient values stored in the CRTM lookup table.
- It is critical to keep the input effective radius consistent with effective radius and water content used to calculate the optical properties for the CRTM lookup table.
- We enhanced the consistency by simplified fitting function derived from the same PSD used in building the lookup table.



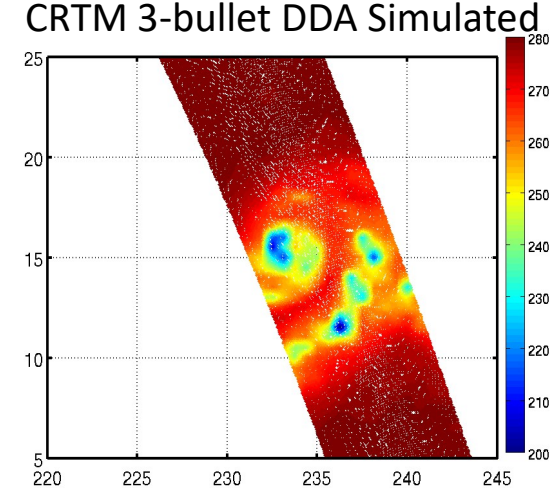
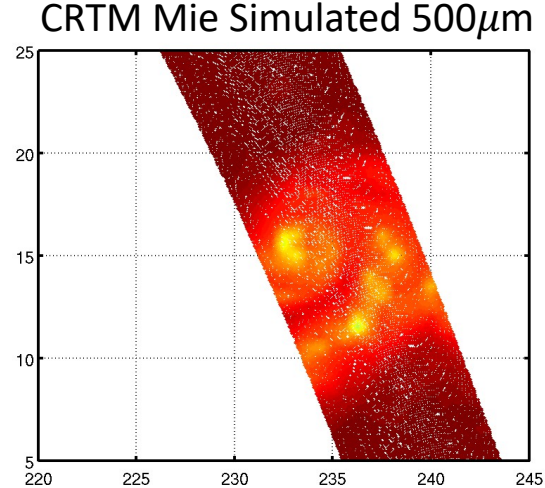
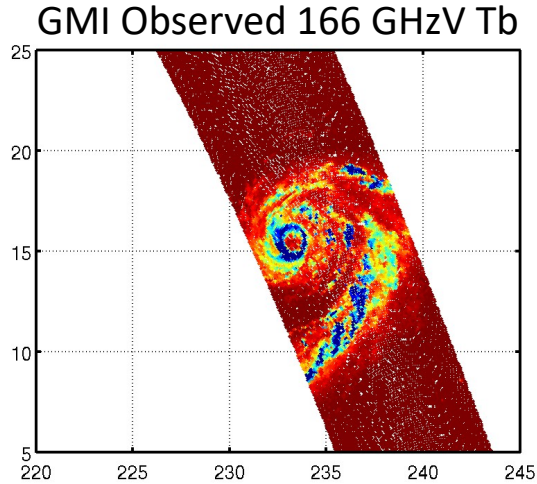


# Monthly Mean of GMI CH10 First-Guess Departures



This slide compares spatial distribution of monthly mean first-guess departures | of GMI channel 10. Non-spherical ice crystal shapes from Liu (2008) and spherical shape were used to generate different sets of first-guess departure data. In general, 3 bullet rosettes produces the smallest mean of absolute first-guess departures and bias among all shapes considered in our current all-sky system.

## Improving Radiance Observation Operator



- Left figure shows the observed GMI brightness temperatures during the hurricane Celina. We can see that very low brightness temperatures were observed GMI instrument near the storms.
- The middle figure shows the computed brightness temperatures using the original CRTM optical properties.
- Right figure shows the computed brightness temperatures using our enhanced CRTM optical properties for microwave instruments.

Comparison of actual and simulated GMI brightness temperature shows results of improved radiative transfer modeling of non-spherical ice crystal shapes

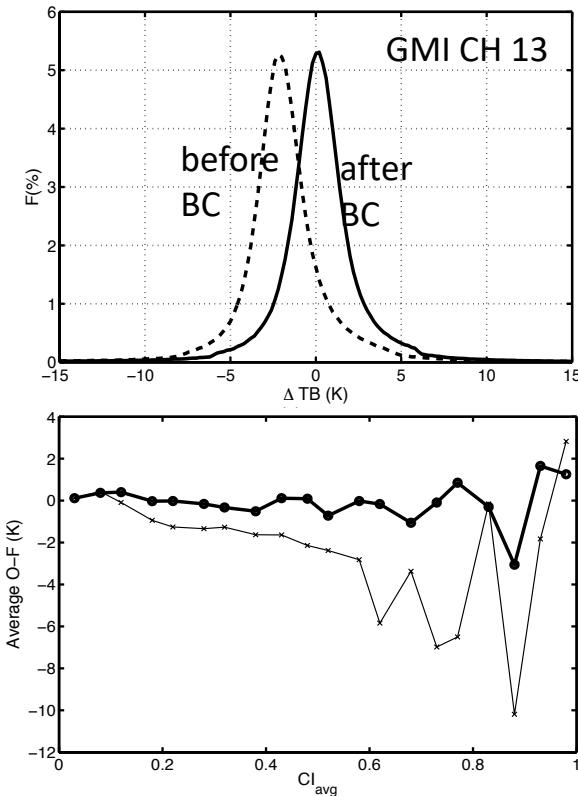
# Quality Control for all-sky GMI radiance data

- All-sky data over ocean with SST lower than 278K were screened out to avoid sea ice affected radiance data.
- Gross check in quality control procedures screen out all-sky GMI data with absolute value of first-guess departure is greater than 2 times of observation error.
- About 24 % of data were screened out after these quality control procedures.

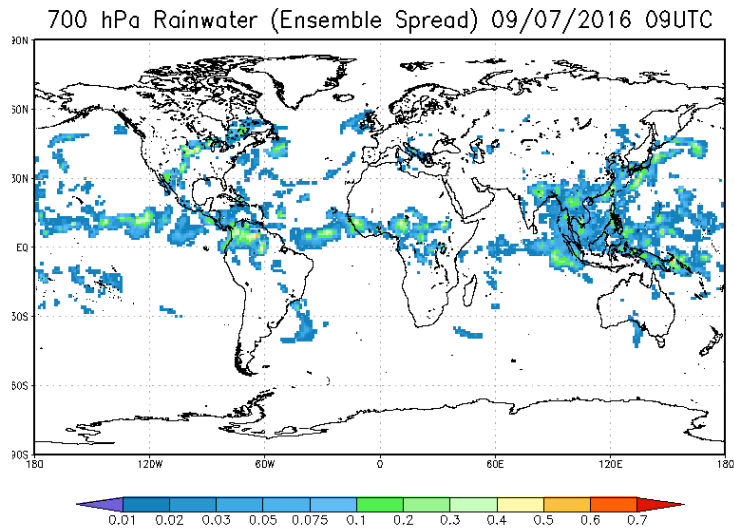
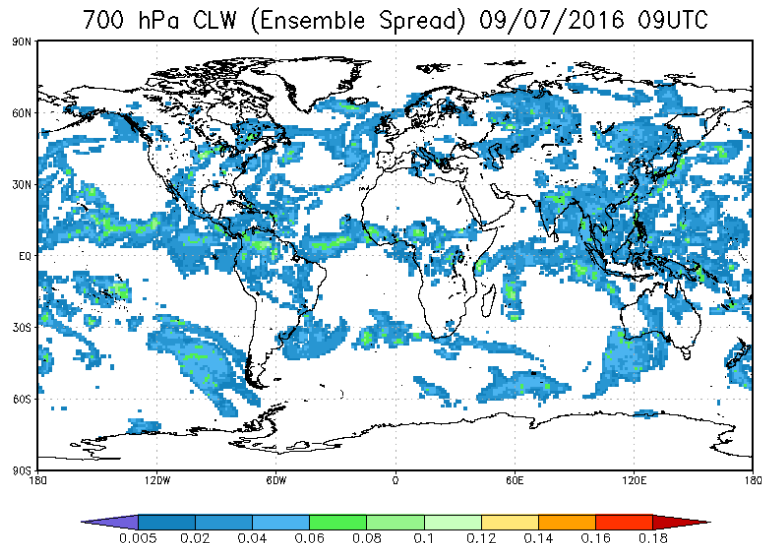
## Bias Correction: VarBC

- **Added cloud index (CI) and  $CI^2$  to the existing bias predictors** (a constant, the scan angle, a second-order polynomial of the atmospheric temperature lapse rate weighted by the radiance weighting function )
- Data used in updating VarBC coefficients were selected. That is, only near-clear sky observations with near-clear sky background profiles and only data where both the observed and simulated cloud indices are greater than 0.05 and their absolute difference is less than 0.005 were used in updating VarBC coefficients.

Thin solid (Thick solid) lines show the biases before (after) using  $CI_{avg}$  as additional predictors in Var BC.

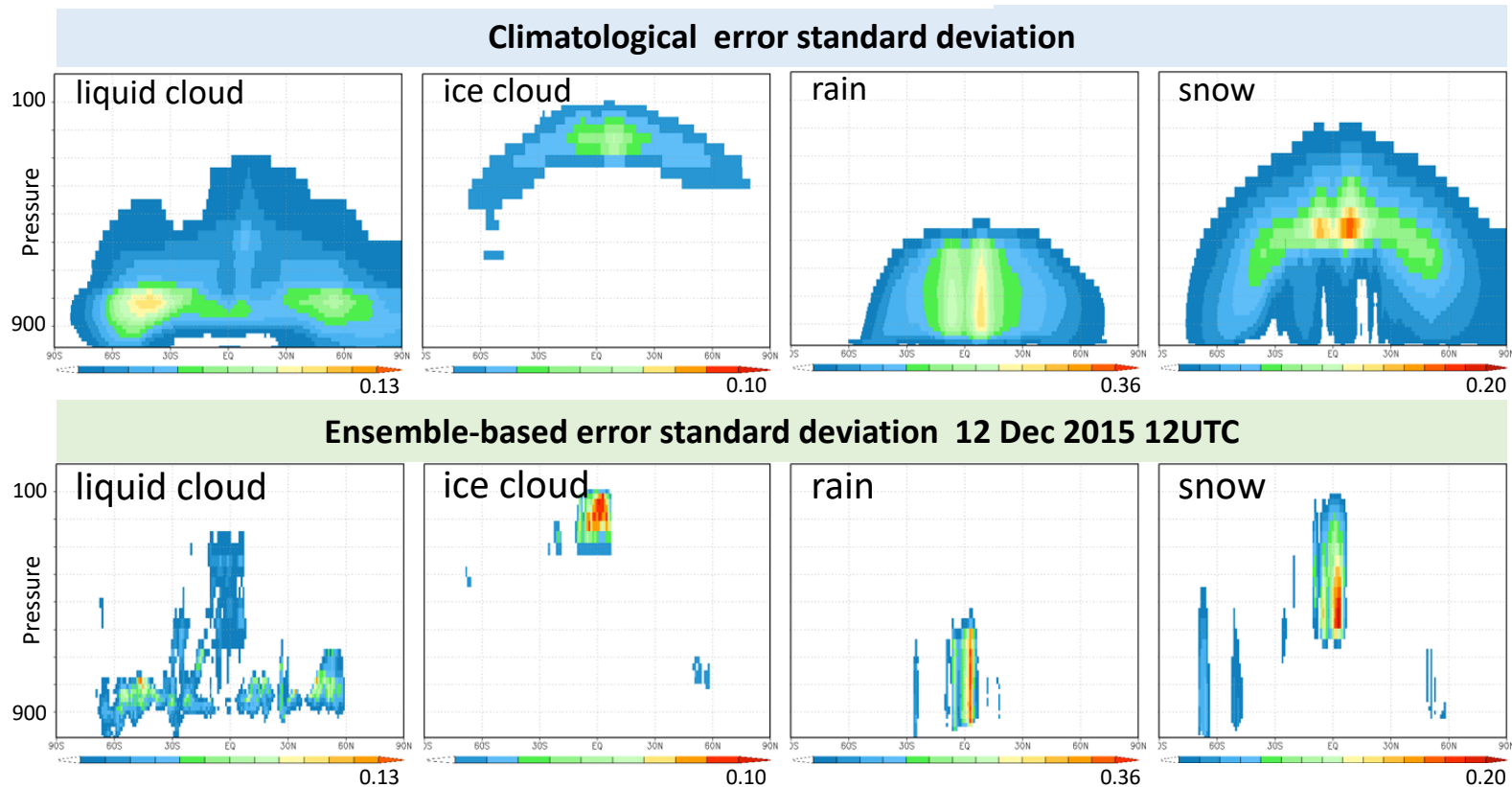


## Ensemble background error for hydrometeors



- 32 ensemble members from GEOS forecasts
- In GEOS-FP, ensemble member forecasts have 0.25 degree resolution, central GEOS forecasts are in 0.125 degree resolution. 72 vertical levels

# Hybrid background errors for hydrometeors



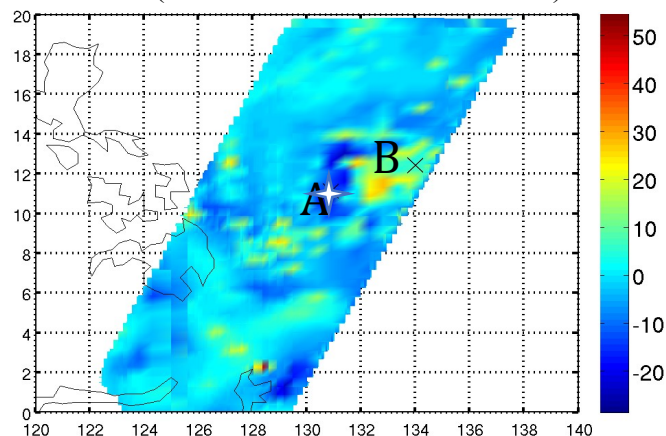
- Figures in the upper panel show the climatological error distribution for liquid cloud, ice cloud, rain and snow. Figures in the lower panel show the ensemble-based error distributions
- Magnitudes of the ensemble background errors are similar to those of the static background errors, although ensemble-based estimates show more detailed flow-dependent structures.
- There are regions with nearly zero ensemble error corresponding to areas where the ensemble members forecasted nearly zero clouds (clear sky). In contrast, the static background errors show nonzero values over broad ranges of latitude.

# Sensitivity to Background Error Covariance: Single Obs Experiment



The full analysis scheme (hybrid 4D-EnVar) was used but only GMI TBs from channels 3-13 are assimilated at a selected single-observation location.

GMI CH6 Tb first-guess departure near Hurricane Melor (1200 UTC 12 December 2015).



Reductions in the first-guess departures for all assimilated GMI channels are largest when pure  $B_e$  is used and smallest when pure  $B_c$  is used. In some cases, the use of  $B_c$  only even deteriorates the analysis results.

	Case A: Departure (K)			
	First-guess	Analysis		
		Pure B <sub>c</sub>	Pure B <sub>e</sub>	Hybrid B
GMI		Pure B <sub>c</sub>	Pure B <sub>e</sub>	Hybrid B
CH3	-23.3	-17.6	-13.2	-15.9
CH5	-13.0	-11.0	-9.2	-10.3
CH6	-17.7	-16.7	-16.0	-16.6
CH10	11.9	11.7	9.1	10.4
CH12	0.68	0.64	0.1	0.4
CH13	3.44	3.3	1.8	2.6

	Case B: Departure (K)			
	First-guess	Analysis		
		Pure B <sub>c</sub>	Pure B <sub>e</sub>	Hybrid B
CH3	43.1	45.1	32.3	43.5
CH5	4.4	5.3	-0.1	4.5
CH6	6.9	6.3	2.5	4.7
CH10	-53.0	-58.7	-45.4	-57.4
CH12	-24.6	-27.8	-22.2	-27.5
CH13	-39.2	-47.1	-33.8	-46.5

# Sensitivity to Background Error Covariance: Single Obs Experiment



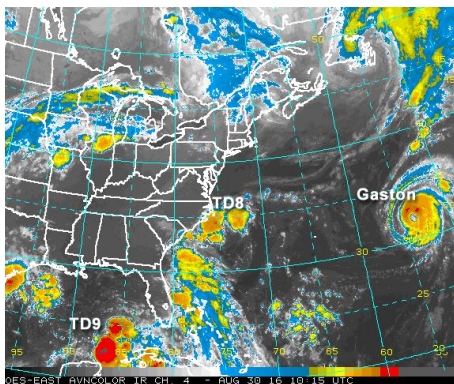
- $B_e$  standard deviations are shown to be larger than those of  $B_c$ , especially for rain water and snow water in the tropical cyclone location selected for the single observation case. Such differences will inevitably be reflected in the analysis increments and on the first guess departures in each of the three background error scenarios.
- The smoothing and time/zonal-averaging needed to produce the static B statistics would render them inadequate for representing error covariances in highly evolving weather conditions; such is the case for the localized and rapidly changing hydrometeors.
- It is worth mentioning here that the difference in the impact is due not only to the difference in the error variances (standard deviations), but also
  - (1) to the localization function/correlation scales (not shown) associated with  $B_e / B_c$  respectively, which control the spatial distribution of the analysis increment, and
  - (2) to the implicit cross-correlations featured in ensemble covariances between the hydrometeors and other variables.

In the current GEOS-FP all-sky data assimilation implementation, we apply only ensemble background error covariance for hydrometeor variables.

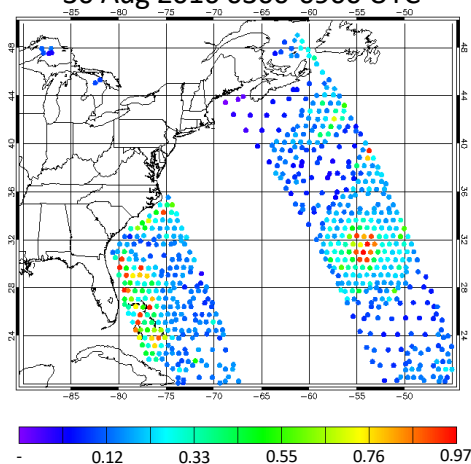
# Dynamic adjustments in precipitating regions



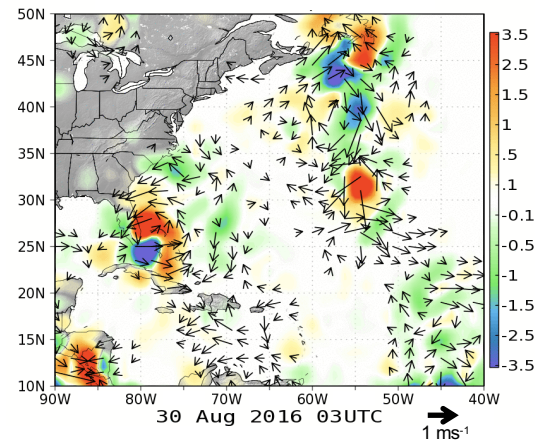
**GOES East IR Imagery**  
30 Aug 2016 1015 UTC



**GMI 37-GHz Tb Polarization Diff**  
30 Aug 2016 0300-0900 UTC



**Analysis Increments 850hpa wind, rain**  
30 Aug 2016 0300-0900 UTC



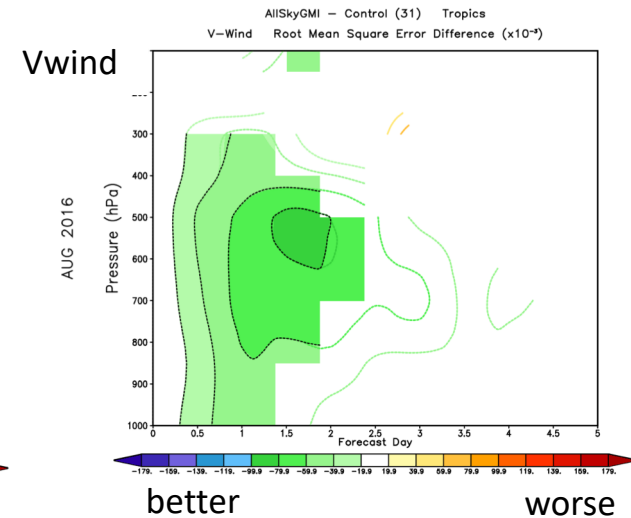
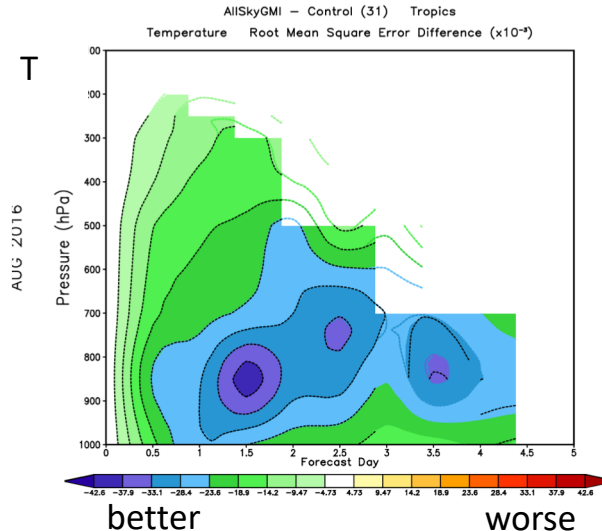
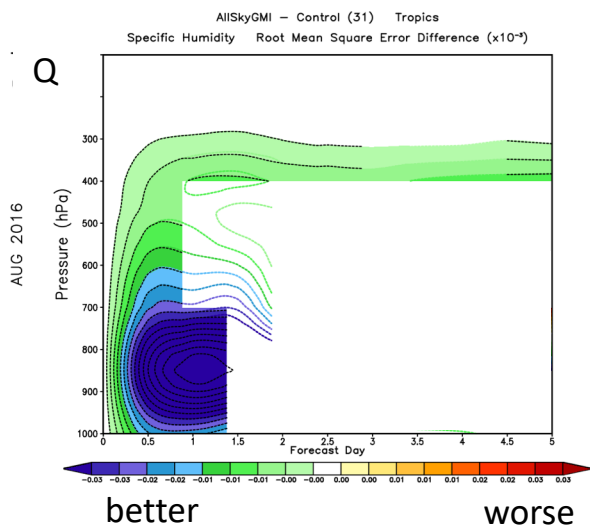
- The ensemble background incorporates correlated errors between different analysis variables implicitly in the GEOS analysis system. Therefore, In addition to hydrometeors, dynamic variables such as wind, temperatures, and pressures are adjusted by assimilating all-sky microwave radiance data in hybrid 4D-EnVar.
- To illustrate that, this slide shows the analysis changes from a simple experiment assimilating only GMI radiance data.
- Figure on the left shows observed GOES East imagery indicating the location of Hurricane Gaston And Figure in the middle shows the observed all-sky GMI data points assimilated in this case study.
- In the figure on the right hand side, color shade shows the horizontal distribution of analysis changes made in 850 hPa rain water mixing ratio by assimilating GMI data. In addition, it is noticed that cyclonic wind changes are clearly generated in the analysis where large precipitation increments are generated near the center of hurricane.
- These changes in both the analyzed moisture and dynamic variables through assimilation of microwave radiance data contribute to GEOS forecast improvements



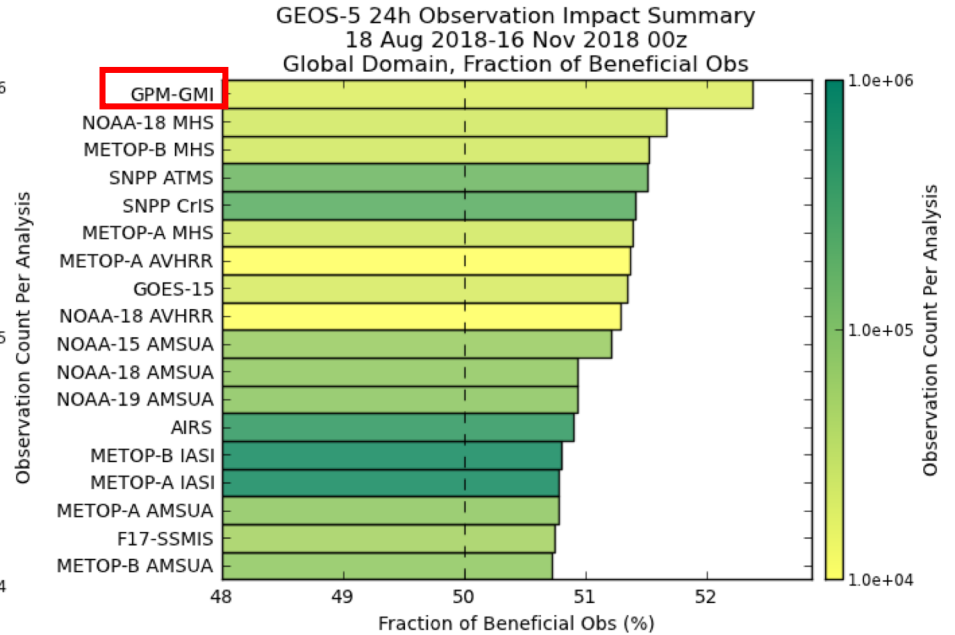
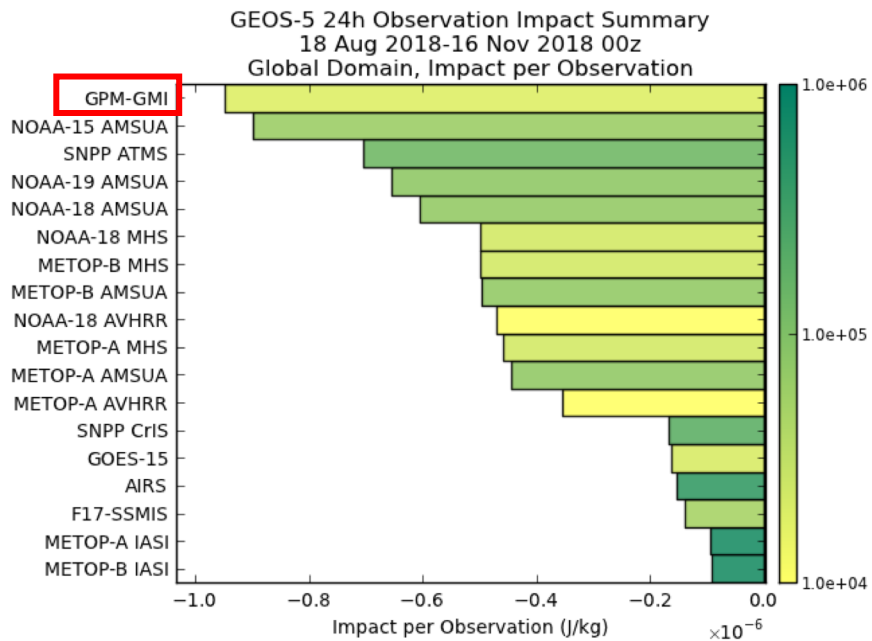
# Impact of GMI all-sky radiances on forecast skill



- The addition of GMI radiances had the largest impact in the Tropics.
- Specific humidity was significantly improved in the short term (0-72 hour) forecasts.
- Similar improvements were seen in mid and lower tropical tropospheric temperature and winds.
- Other modeling and initialization improvements included in the FP upgrade retained these improvements into the medium range.



# Forecast Sensitivity and Observation Impact (FSOI)



- The GMI improvement is consistent with results seen via the FSOI metric which measures each observation impacts on 24 hr forecasts.
- GMI is seen to have the highest impact per observation of all the radiance observation types despite their relatively low number of observations.

# Extending All-sky DA System to Other MW radiance Data for future GEOS-FP upgrades and next MERRA reanalysis



## Status of all-sky MW data assimilation developments in GEOS

Satellite	Sensor (Scanner)	# of Channels (Frequency)	Clear sky		Cloudy/Precipitating sky	
			Ocean sfc	Non-Ocean	Ocean sfc	Non-Ocean
GPM	GMI (conical)	13 channels (10GHz~190GHz)	★	★	★	★
GCOM-W1	AMSR-2 (conical)	7 channels (6.9 GHz ~ 89 GHz)	★		★	
DMSP F16, F17, and F18	SSMIS (conical)	24 channels (19.35 GHz ~ 190GHz)	● ★	● ★	★	★
NOAA-18 & 19, METOP-A & B	MHS (cross-track)	5 channels (89GHz ~ 190GHz)	● ★	● ★	★	★
NOAA-18 & 19, METOP-A & B	AMSU-A (cross-track)	11 channels (23.8 GHz ~ 89 GHz)	● ★	● ★	★	★
SNPP, NOAA-20	ATMS (cross-track)	22 channels (23.8 GHz ~ 190GHz)	● ★	● ★	★	★
Megha-Tropiques	SAPHIR	6 channels (183.2 GHz ~ 194.3GHz)	★	★	★	★



Clear-sky assimilated in GEOS-FP



All-sky data assimilated in GEOS-FP



To be implement in GEOS-FP later this year



Development getting matured.



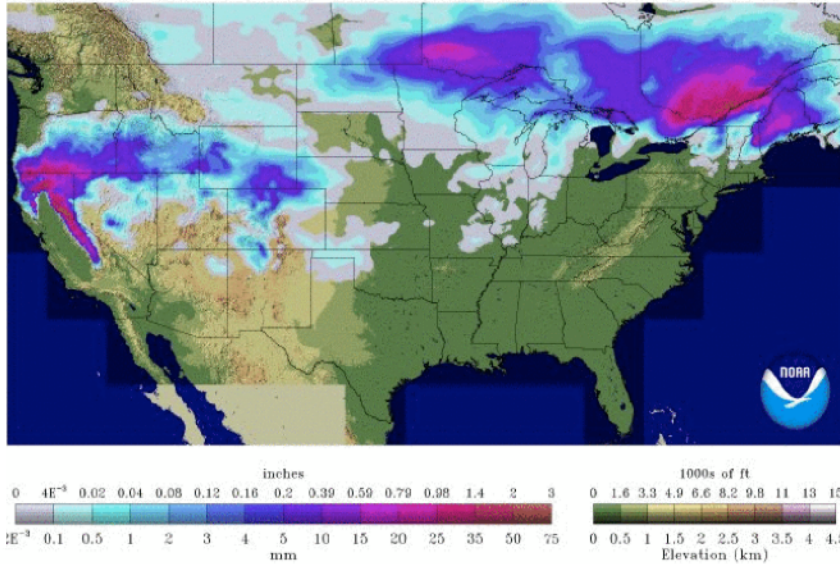
Development has just started.

# Extending All-sky DA System to Other MW radiance Data for GEOS-FP upgrades and next MERRA reanalysis

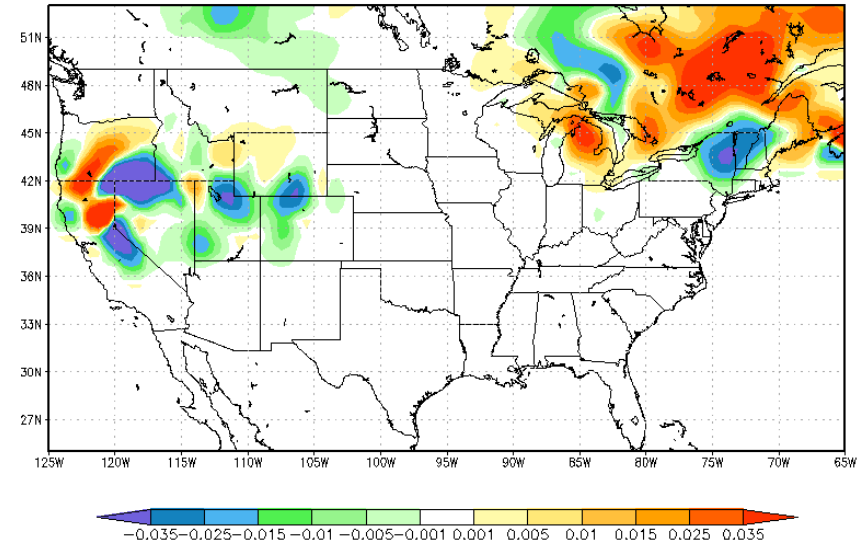


## Early January 2017 North American Winter Storm

Observed 24 hour total snow precipitation



Snow precipitation analysis increments by assimilating all-sky GPM + MHS data

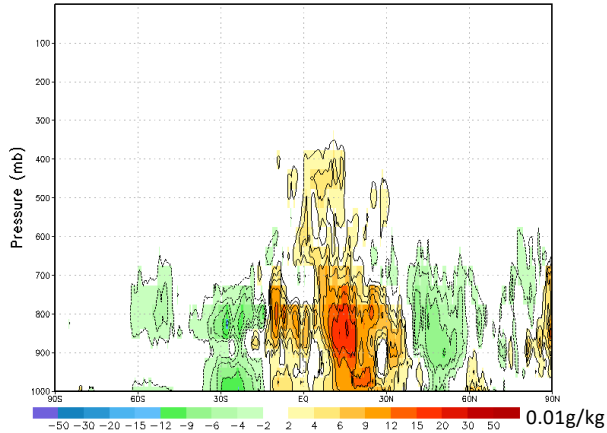


- This slide illustrates precipitation analysis increments from all-sky microwave data from GPM and several NOAA and European satellites. Left figure shows the observed 24 hourly snowfall accumulation during the 2017 January North America Winter Storm that affected large are of US from west to south to east. Right figure shows the falling snow precipitation changes by assimilating all-sky data from GPM microwave imager and several Microwave Humidity Sounders and demonstrating these extended all-sky data can adjust snow precipitation in the analysis to be much closer to the observations. Other atmospheric parameters like water vapor and surface pressure are also adjusted physically consistent manner and demonstrated improvements in GEOS forecast skills.

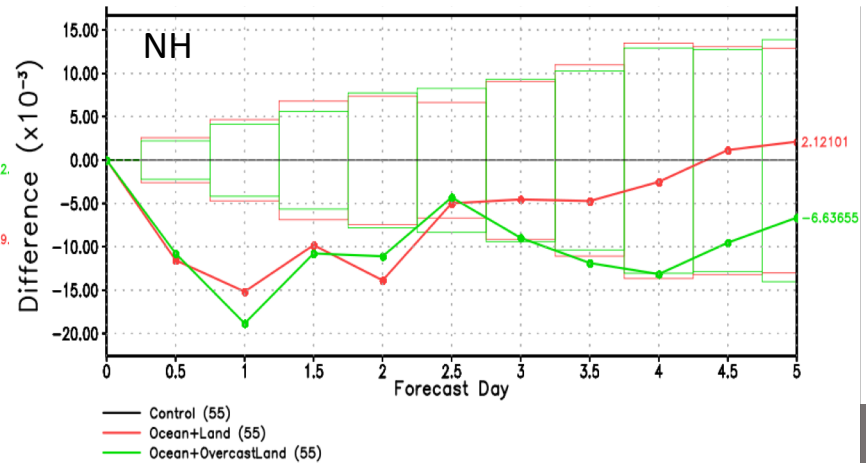
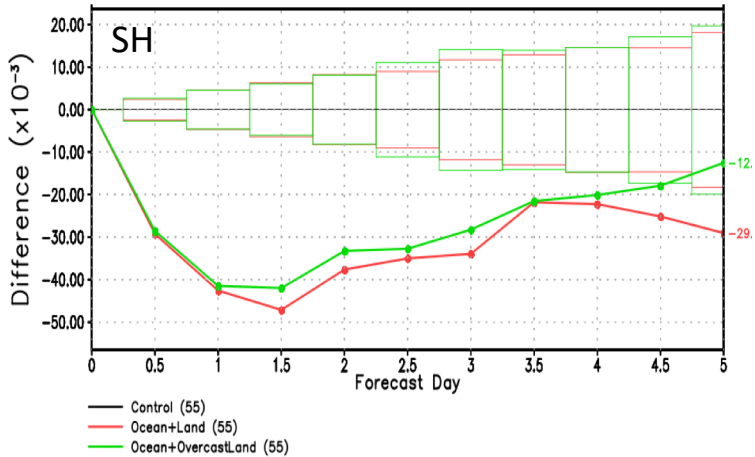
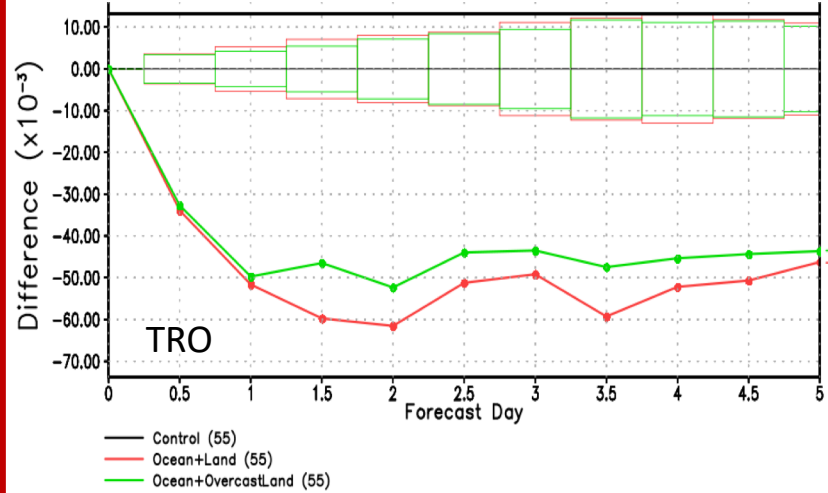


# Impact of MHS all-sky radiances on GEOS analyses and forecasts

July 2018, Monthly Mean Qv Analysis Difference  
AllskyMHS - CNTL



Forecast Error Reduction  
850 hPa Humidity RMSE Difference



# Summary

- GMAO has implemented all-sky GPM Microwave Imager (GMI) data assimilation in GEOS FP, increasing not only the number of satellites observations assimilated but also the types of variables analyzed.
- All-sky GMI data made significant positive Impacts on GEOS forecasts especially for lower tropospheric water vapor, temperature, and winds.
- All-sky techniques in GEOS are currently being extended to other microwave sensors such as MHS, ATMS, AMSU-A, and AMSR-2. NWP experiments assimilating all-sky MHS and all-sky AMSR2 demonstrated significant reductions in GEOS forecasts errors and plan to be included in the GEOS-FP upgrade later this year.
- We plan to utilize TMI, GMI, and other satellite microwave radiance observations for future GMAO reanalysis.

## Work Plan

- Switch to latest CRTM (v2.3.0) and test with cloud fraction consideration in observation operator
- Test Inter-channel correlation of observation errors for all-sky microwave radiance data
- Examine optimal thinning distances for cloudy area and include in the future all-sky system.
- Incorporate particle size information from the GEOS two moment moisture physics schemes in building CRTM lookup tables and CRTM radiance simulations.